Ultrasound measurements in a physical model of Czochralski crystal growth in a horizontal magnetic field

Josef Pal[1], Ilmars Grants[1,2], Sven Eckert[1], and Gunter Gerbeth[1]

[1] Helmholtz-Zentrum Dresden-Rossendorf, Bautzner Landstr. 400, 01328 Dresden, Germany
[2] Institute of Physics, University of Latvia, Salaspils, Latvia

A horizontal magnetic field (HMF) may improve conditions in the melt during large silicon single crystal growth by the Czochralski technique. This observation is counter-intuitive as the HMF evidently breaks the rotational symmetry. A previous study has shown that the HMF is not able to significantly delay the Rayleigh-Bénard instability in a rotating cylinder. It has been observed that an oscillating flow sets in soon after the linear onset. Can we expect a stabilizing effect of the HMF in the Czochralski growth? Why the symmetry breaking by the HMF is eventually not so relevant? These are two central questions for our primarily experimental study. Besides, it is also meant as a benchmark for comparison with the numerical codes. To serve the latter purpose the boundary conditions should be preferably well defined. Having this in mind the temperature boundary conditions are defined as follows. An isothermal heating is applied at the bottom of a cylindrical cell filled with GaInSn alloy. The side wall is thermally insulated. An optionally rotating isothermal cooler models the growing crystal. A water-cooled layer of an alkaline solution keeps the rest of the metal surface free from oxides and models the radiation heat loss. The maximum HMF strength is 0.3 T that corresponds to a Hartmann number of about 1200. Velocity profiles are measured by ultrasound Doppler velocimetry.

Keywords: Czochralski crystal growth, Horizontal magnetic field, Ultrasound Doppler velocimetry

1. Introduction

HMF has emerged as one of the most promising magnetic field configurations in the single crystal silicon growth by the Czochralski (CZ) technique. Various numerical simulations of the process [1, 2] have shown that HMF strongly stabilizes the melt under characteristic growth conditions. This observation contrasts with the linear instability results [3] in a cylindrical Rayleigh-Bénard (RB) cell predicting onset far below the typical CZ conditions. The linear instability is monotonic that means another steady solution sets in. Such instability by itself is practically harmless in the sense that it brings no instationarity. However, it is known from experiments in a rectangular RB cell [4] that the first linear onset is soon followed by secondary instability which leads to oscillating flow. One of the main tasks of our study is to address this apparent contradiction in a physical model of the CZ process with HMF.

The RB cell is a rough model of CZ focused on the basic instability driving mechanism by unstable stratification of the melt. One of the key differences between RB and CZ configurations is the intrinsic radial temperature gradient in the latter. This gradient drives a flow in the CZ melt for an arbitrary small temperature gradient. This flow should be proportional to the driving buoyancy force (temperature gradient) when it is small enough. In the RB, in turn, the flow is zero unless the linear instability creates it at a sufficiently high temperature gradient. One may expect that instead of instability the CZ melt will develop a flow regime with a faster-than-linear dependency of velocity vs the temperature gradient. This "ghost" of the linear instability is another target of our study.

Instationarity may be produced in the CZ process also by a completely stable three-dimensional flow. A stationary but non-uniform azimuthal distribution of velocity and temperature in the melt produces oscillating conditions on the surface of a rotating crystal. The HMF evidently breaks the rotational symmetry. It is, therefore, puzzling how it may produce satisfactory growth conditions. In the current study we consider only a stationary crystal that can hardly solve this puzzle. The measurements are more intended to quantify the maximum initial degree of the azimuthal non-uniformity of the flow in the bulk of melt. These results should serve as an input for the design of further model experiments with HMF and the crystal rotation.

2. Basic principles in modelling the Czochralski technique

The simplest model of the CZ facility might be a RB configuration, in particular a cylindrical cell heated from below and cooled at the top which is characterized by a height H and diameter $2R$ and adiabatic insulated side walls. Applying a temperature gradient $\Delta T = T_b - T_t$ between the bottom and top sides, buoyant convection occurs when ΔT exceeds some critical value.

The dynamics of the mere thermally induced convection may be described by three control parameters. First of all the dimensionless Rayleigh number Ra is the crucial parameter in modelling buoyancy and describes its strength: $Ra = \beta g \Delta T H^3 / \nu \chi$, where β is the thermal expansion coefficient , ν the kinematic viscosity, χ the thermal diffusivity of the fluid, and g the gravitational acceleration. The second control parameter, the Prandtl number Pr, takes into account the heat transport within the fluid and is given by the ratio of the thickness of viscous and thermal boundary layers: $Pr = \nu / \chi$. In general, molten metals and semiconductor melts are low Prandtl number fluids with Pr in the order of 10^{-2}, which

means that the heat diffuses quickly in comparison with the convective transport.

The third control parameter, the aspect ratio $a = H/(2R)$ concerns the geometry of the setup and affects crucially the developed convective pattern inside the melt. More details, in particular about varying aspect ratios, can be found in [5, 6] and references therein. The initial filling level in a real industrial CZ facility does not reach $a = 1$, it is even lower than $a = 0.5$ and decreases continuously during the process.

The Hartmann number $Ha=BL(\sigma/\rho\nu)^{1/2}$ occurs as another control parameter if external magnetic fields are exposed to the system. Thereby B is the magnetic induction, L a typical length scale in the system, and σ the electrical conductivity of the melt. The Hartmann number represents a measure for the ratio between the electromagnetic body force and the viscous force.

3. Description of the model

The object of the investigation is a modified Rayleigh-Bénard (RB) configuration, a cylindrical melt column of variable aspect ratio homogeneously heated from below. The photo in Fig. 1 illustrates the experimental setup mounted between the HMF producing coils. As working fluid the ternary alloy GaInSn [7] was used because it remains liquid at room temperature and as distinguished from mercury it is non-poisonous. Moreover, its low Prandtl number is similar to that of molten silicon.
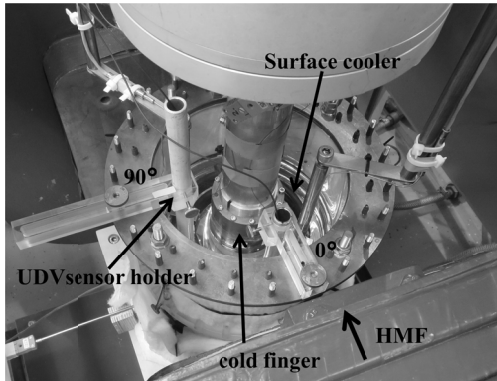

Figure 1: Oblique view to the experimental setup mounted inside the HMF coil system. The inner diameter of the cylindrical melt volume is 178 mm whereas that of the cold finger is 70 mm.

The heating was realized by an electrical heating plate embedded in a massive copper disc to achieve isothermal boundary condition. Several thermocouples were installed inside the copper disc to monitor its temperature. The upper thermal boundary condition in a CZ system is accounted for by a partially cooled surface. The partial cooling in our experiment covers approximately the same fraction area as the crystal does in an industrial facility. It is realized with a circular heat exchanger (cold finger) mounted concentrically at the top of the experimental cell. The cold finger is optionally rotable, a precise control of the temperature is realized by supplying it with coolant fluid at high flow rate from a thermostat having a large reservoir. The latter is regulated

by a PID circuit. The temperature of the cold finger is also monitored at various positions. For the purpose to achieve adiabatic boundary conditions at the side walls a borosilicate glass pipe was chosen as experimental cell owing to its poor heat conductivity. During the measurements, the apparatus was embedded in mineral wool to minimize the lateral heat loss.

In the industrial Czochralski facility thermal radiation from the hot silicon melt surface to the ambience is a considerable heat sink. A distinctive feature of the present setup is the possibility to model the heat loss from the melt surface. The surface is therefore covered by an electrolyte layer which is cooled by a copper spiral completely immersed into this layer (cf. Fig. 1). Such a system can be described by the dimensionless Biot number Bi. For a detailed meaning of this dimensionless heat transfer coefficient [8] is referred to.

Flow velocities were measured by the UDV technique, the principle of operation is described in the pioneering work of [9]. Mainly two features render UDV predestinated for the present work. Firstly, it works for opaque media including liquid metals. Secondly, it allows the quasi-simultaneous measurement of an entire profile of the local velocity component in direction of the sound propagation along the ultrasonic beam. The readings of the ultrasound transducers were taken by a DOP2000 velocimeter (Signal-Processing, Lausanne, Switzerland).

A simplified numerical model has been used for comparison purposes. It is implemented as the spectral three-dimensional time-dependent direct numerical solution developed for the linear instability analysis in the RB cell [3]. The flexibility of this model is restricted by boundary conditions that must be of a fixed type on each of the principal surfaces (bottom, side, top). This introduces a difficulty to model the top surface consisting of two distinct regions. The central part below the cold finger has no-slip conditions for the velocity field and, effectively, a constant temperature. The outer part, in turn, has stress-free conditions for the velocity and boundary conditions of the third kind for the temperature. Since the area of the cold finger is much smaller than the area of the free surface the latter conditions are applied for the entire top surface:

$$\left(\frac{\partial v_\tau}{\partial z}\right)_{z=1} = 0 \text{ and } \left(T + Bi^{-1}\frac{\partial T}{\partial z}\right)_{z=1} = T_e(r).$$

The ambient temperature profile is set to $T_e(r) = -1/8 + 3/2\,T_2(r) - 3/8\,T_4(r)$, where $T_i(r)$ are the Chebyshev polynomials used to express the numerical solution [3]. The value of Biot number is set to Bi=2. The above boundary conditions constitute the basic deviation from the physical model.

4. Results

For the present investigation mainly flow velocity measurements were performed in the range $Ra=[10^4:10^7]$ and different magnetic fields $B=[86, 160, 326]$ mT which correspond to the Hartmann numbers $Ha=[300, 600, 1200]$. The cell filling height was kept constant at $H=89$ mm and results in an aspect ratio of $a=0.5$. To measure

the vertical velocity component two UDV sensors were positioned 25 mm away from the rim of the cylinder. Since the HMF breaks the rotational symmetry, one of the sensors was in the plane parallel ($\varphi=0°$) to the HMF direction, the second one in the plane perpendicular ($\varphi=90°$) to the HMF (see Fig. 1).

Fig. 2 shows exemplarily a selection of the experimentally and numerically determined mean velocity profiles at both distinguished positions for $Ha=300$. Why the numerical data do not reproduce quantitatively very well the experimental ones might have several reasons, such as the modeling of the thermal boundary condition by the Bi number. This is still under development. On the other side, see Fig. 2b, for the higher Ra the curvature of the velocity profile is quite good reproduced with both local maxima.
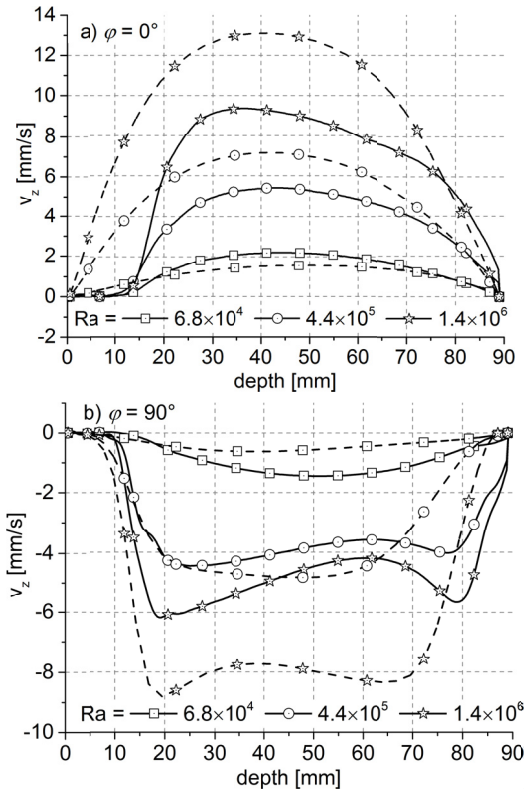

Figure 2: Experimental (solid lines) and numerical (dashed) vertical velocity profiles for $Ha=300$ for selected Ra. Profiles with positive sign (a), indicate a downward oriented flow and the negative sign in (b) stands for upward flow direction.

For further comparison purposes the dimensionless velocity expressed by the Reynolds number Re is useful which gives the ratio of the inertial to the viscous forces. Here Re is calculated from the maximum v_z value of the velocity profile by $Re=v_{z,max} R/\nu$. Fig. 3 summarizes Re as function of Ra and of Ha, and shows, additionally, a comparison with first numerical results. For $Ha=300$ the experimental results are interesting because the average velocity decreases as the heating power increases for $Ra>4.8\times10^6$ ($\varphi=90°$) and $Ra>5.5\times10^6$ ($\varphi=0°$), respectively. This is probably because of roll movement and requires more attention in subsequent investigations.
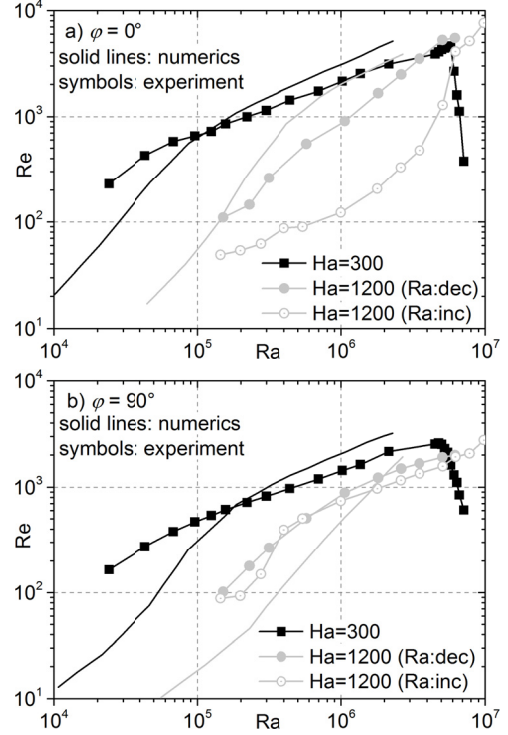

Figure 3: Comparison between the experimental and numerical Re as function of Ra for two different Ha numbers.

A kind of velocity "boost" is observed in the numerical results shown in Fig. 3. This cannot be validated by the experiment because of the limited resolution of the UDV technique. Velocities lower than approximately 1 mm/s (which correspond in the present setup to $Re \leq 260$) are hardly measurable and depend extremely from the UDV signal quality. For $\varphi=0°$ a distinct hysteresis behavior is observed for $Ha=1200$ depending from the ramp direction by varying the Ra number. The symbols with open circles indicate the case when Ra was increased, the filled ones are for decreasing Ra. The difference is small for the lower Ra range, but a difference of almost one order of magnitude occurs for around $Ra=10^6$.

Concerning the spatio-temporal behavior of the flow for $Ha=300$, the measurements show signs of different oscillation mode competitions. First of all Fig. 4 shows the cases before instabilities develop. First instability comes with an oscillation frequency of $f=0.123$ Hz at $Ra=2.1\times10^6$, disappears and a low frequency oscillation with $f=0.071$ Hz occurs at $Ra=2.6\times10^6$. Increasing further the Ra number this oscillation mode stops too and a high frequency mode starts from $Ra=3.1\times10^6$ up to $Ra=5.1\times10^6$ with slightly increasing frequency between $f=0.221$ Hz and $f=0.281$ Hz, respectively. In the latter range, interestingly, the oscillations are only present for $\varphi=90°$. For Ra between $[5.3\times10^6...5.8\times10^6]$ the oscillations disappear again but restart with a very low frequency and large amplitude at $Ra=6.1\times10^6$ for up to $Ra=6.7\times10^6$. The spatio-temporal process in Fig. 5 illustrates this behavior, whereas Fig. 6 shows the time variation of the vertical velocity at some selected deeps of the melt column. It can be seen that higher amplitude oscillations occur for $\varphi=0°$ than for $\varphi=90°$. For the

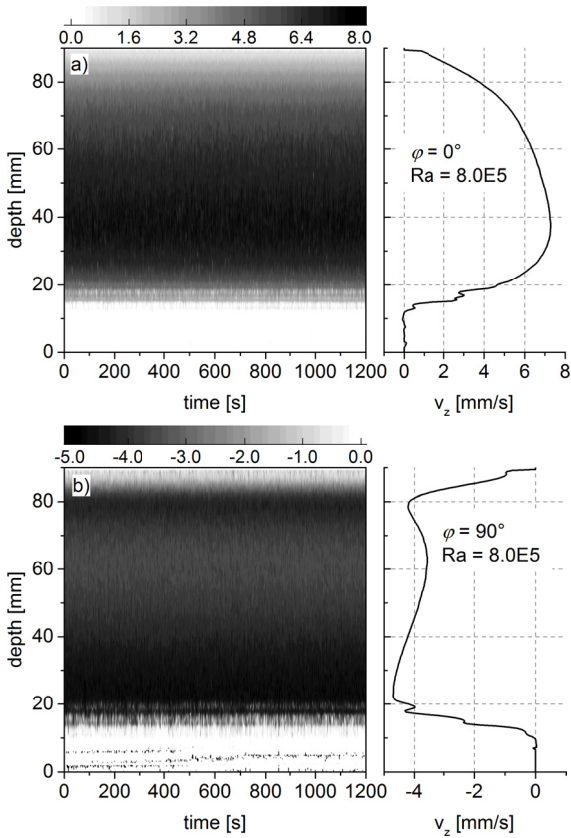highest measured $Ra=7.1\times10^6$ the oscillations broke down and an irregular flow structure was observed.

Figure 4: Time series and the mean profile of the vertical velocity measured at the $\varphi=0°$ (a) and $\varphi=90°$ (b) positions. Yet, no oscillations are observed for $Ra=8\times10^5$.

5. Summary

A CZ-like crystal growth model exposed to a HMF was the object of the present investigation. Ultrasound measurements of the vertical component of the fluid flow were performed by varying the strength of the magnetic field (Ha) and that of the buoyancy (Ra). Because the HMF breaks the rotational symmetry the velocities were recorded at two distinct azimuthal positions. The experimental data serve as a benchmark object for numerical codes which are still under development.

6. Acknowledgements

References

[1] V. V. Kalaev, J. Cryst. Growth 303 (2007), 203–210.
[2] X. Chen, J. Zhan, Y.-S. Li, X. Cen, J. Cryst. Growth 389 (2014), 60–67.
[3] I. Grants, G. Gerbeth, J. Cryst. Growth 358 (2012),43–50.
[4] U. Burr, U. Müller, J. Fluid Mech. 453 (2002), 345–369.
[5] F. Hébert, R. Hufschmid, J. Scheel, G. Ahlers, Phys. Rev. E 81 (2001), 046318.
[6] J. Niemela, L. Skrbek, K. Sreenivasan, R. Donnelly, J. Fluid Mech. 449 (2001), 169–178.
[7] Y. Plevachuk, V. Sklyarchuk, S. Eckert, G. Gerbeth, R. Novakovic, J. Chem. Eng. Data 59(3) (2014), 757–763.
[8] J. Pal, A. Cramer, I. Grants, S. Eckert, G. Gerbeth, J. Cryst. Growth 432 (2015), 69-77.
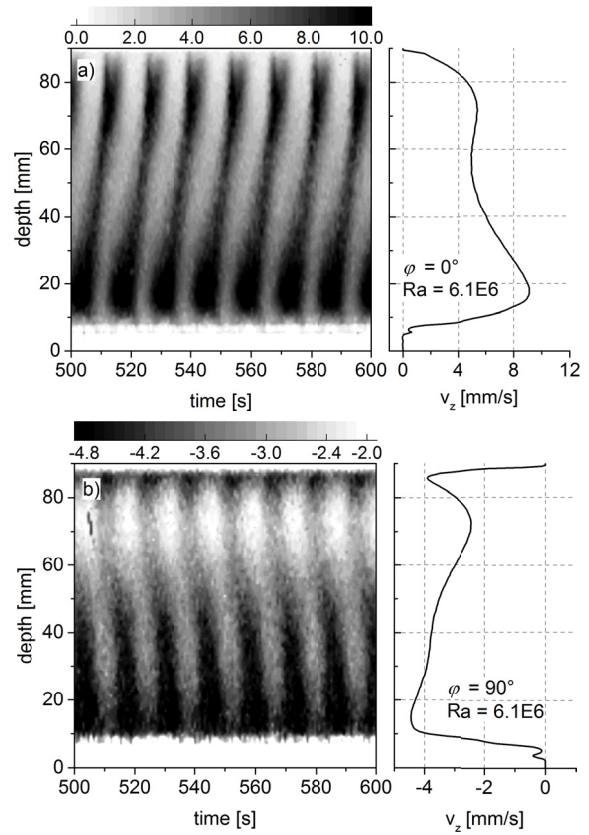[9] Y. Takeda, Nucl. Eng. Des. 126 (1991), 277-284.

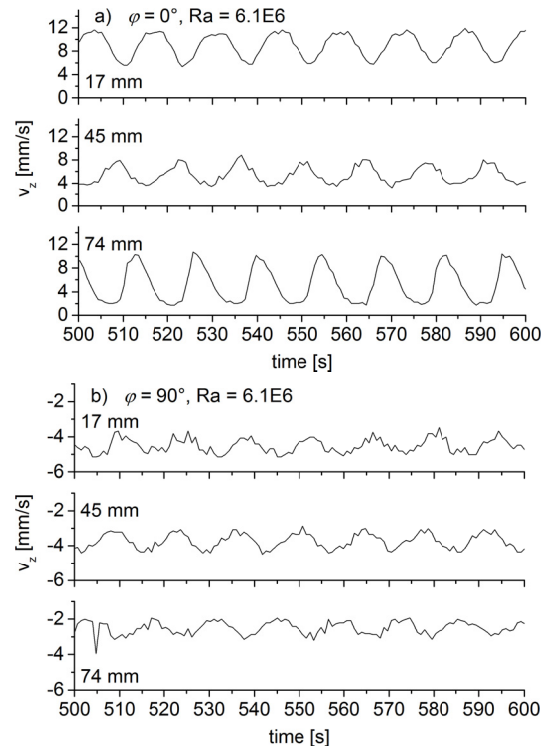Figure 5: Low frequency and large amplitude oscillations ($f=0.073$ Hz) for $Ra=6.1\times10^6$.

Figure 6: Time variation of the vertical velocity as shown in Fig. 5 at selected deeps of the melt, (a) $\varphi=0°$ and (b) $\varphi=90°$.